

The role of interparticle contact in conductive properties of random particulate materials

Y.B. Yi

Department of Mechanical and Materials Engineering, University of Denver, 2390 South York Street, Denver, CO 80208, USA

Received 10 December 2007; received in revised form 9 February 2008; accepted 11 February 2008

Available online 14 March 2008

Abstract

The effective conductivity of material systems consisting of contacting particles is studied computationally using a model of mono-disperse circular disks. The electrical or thermal conductivity is computed by modeling the relevant mechanical contact problem followed by a steady-state conduction analysis. The interparticle contact resistance is incorporated via the introduction of gap conductance in the contact pairs. Monte Carlo simulations show that the overall effective conductivity is much lower than that predicted by the model using an overlap assumption, even when the contact resistance is zero. The results also display a nonlinear relationship between the contact resistance and the effective conductivity. Therefore, in practical applications involving particulate inclusions of high density, the interfacial contact must be considered to reliably predict the relevant transport properties. Although the methodology is developed in the context of circular disks, it can be extended to deal with more general situations.

© 2008 Acta Materialia Inc. Published by Elsevier Ltd. All rights reserved.

Keywords: Electrical properties; Thermal conductivity; Monte Carlo techniques; Modeling

1. Introduction

Heterogeneous particulate or fibrous materials are of importance in many applications in modern industry and in scientific research [1,2]. In designing materials containing various shapes of particles or fibers, which can be viewed as high aspect-ratio particles, the conductive or percolation properties are often of major concern. Earlier work in this area involved the application of effective medium theories, which can provide qualitative trends on the behavior of the effective properties in some special cases. However, they cannot be quantitatively predictive for general situations involving random dispersions [3]. The fact that the predicted conductivity or percolation threshold using the effective medium theories were not in agreement with experiments at lower volume fractions has been well documented [4,5]. In addition, there has

been a variety of studies on the prediction of physical properties of composite materials using homogenization methods [6,7]. However, these analytical approximations or other semi-empirical approaches to the problem have been shown have difficulties in most situations [8]. A more general strategy for the problem is to employ Monte Carlo simulation techniques. In early work, Kirkpatrick's simulations [9] indicated that the percolation threshold, i.e. the density or volume fraction of the material phases at percolation onset, exhibited a power-law dependence on bond fraction. This power-law relation was also found to hold for conductivity in more general material systems [10,11]. Pike and Seager [12] also examined conduction and percolation phenomena in stick or disk networks, using two- and three-dimensional Monte Carlo simulations. The effects of hardcore interactions, probabilistic and deterministic bonding parameters, and various forms for the bonding function were specifically investigated.

These theories and methodologies have recently been implemented in many applications, including the prediction

E-mail address: yyi2@du.edu

of the conductivity of graphite particles in Li-ion electrode materials, in which a higher electrical conductivity is desired to reduce the irreversible capacity loss [13,14]. It has been shown that increases in electronic or thermal conductivity may be achievable by compression of anodes into higher volume fraction plates [15,16]. Simplified models assuming the overlap geometries were used to predict the effective conductivity of the graphite particles. In these models, when the spatial locations of some portions of two particles coincided, they were simulated as a merged joint at their original locations. Therefore the resistances between the contact surfaces were not considered. During the mixture and compression processes in manufacturing, however, mechanical deformations along the contact surfaces of particles can occur, and particularly when impermeable coating layers or rough surfaces are involved, the contact resistance will be appreciable. If the interparticle contacts were ignored in the model, the computed effective conductivities would be overestimated compared to the actual values. The significant discrepancies were indeed observed in the experiments compared to the theoretical predictions that assumed an overlap [14].

In carbon nanotubes, the fibrous networks formed by nanoscale tubes have traditionally been simplified as two-dimensional line segments [17] or three-dimensional overlapping cylinders [18,19]. The joint morphology at the inter-tube connections has also been investigated in detail to inform simulations of two-dimensional networks [20]. These models were more or less successful in predicting the trend in the bulk properties. However, the assumption of overlapping geometry or fillet-shaped joint morphology is in fact questionable when the physical contact takes place between the carbon atoms on the tube walls. In fact, it was found that the predicted properties for nanotube sheets assuming overlapping solid fibers could be an order of magnitude different from the results actually measured [18]. Although opinions in the research community vary, it is believed by the author of the current work that the interfacial geometry assumption must be modified to include contact situations in the relevant computations.

Study of the interfacial effects on the effective transport properties of composite materials is not new. For example, Torquato and Rintoul [21] developed rigorous bounds on effective conductivity for the interfacial surface effect between spherical inclusions and matrix. The technique was based on the trial field solutions of the single-inclusion boundary value problems. This work was later extended by some researchers for solving other problems as well, including Miloh and Benveniste [22], who studied the effective conductivity of composite media with ellipsoidal inhomogeneities and highly conducting interfaces; Wei and Poon [23], who studied the graded composites with cylindrical inclusions with heat contact resistance; and Benveniste [24], who developed a general interface model for an arbitrary three-dimensional curved interphase between two anisotropic solids.

These models deal with two- or three-phase composite material systems, in which both the particles and the matrix material are conductive and the particles do not touch one other. Therefore the term “interface” has been defined as the contact surfaces between the inclusions and the matrix media. In addition, the inclusions are assumed to be completely bounded by the matrix and the contact area is the entire surface of an inclusion. The problem studied in this research, however, is physically different from all these models in that a single-phase material system is investigated. The matrix is assumed to be a nonconductor and the volume fraction of particles studied here is close to or above the maximum packing limit of the corresponding rigid particle systems, so that the conductive paths are always formed by the contacting particles alone. Therefore the term “interface” here is referred to as the common surface formed by two particles in physical contact. As a consequence the contact area is variable and generally much smaller than the entire surface area of a particle. The nonlinearity in the problem is induced by the nonlinear relationship between the contact area and the contact pressure. In contrast, in the effective medium theories, the nonlinearity is primarily a result of solving the Laplacian equation in multiphase composite media without considering the contact mechanics.

The goal of the current research is to study the effect of the interparticle contact resistance on the effective conductive properties, via Monte Carlo simulations and finite element approaches. A representative shape of particles, i.e. a disk, will be used throughout the study. Although a dynamic contact model has previously been developed by the author to study the stress concentration and the packing limit for random ellipsoidal particles [25], the research work relating to the conductive properties of similar material systems is not yet available in the literature. The current work aims to extend the existing mechanical compression model and allow the modeling of the associated transport properties. This is by no means a trivial extension, because solving the problem, requires handling not only the relevant contact mechanics, but also the electrical or thermal problems. The multiphysics coupling mechanisms require a new modeling and simulation technique.

In addition to the mechanical contact, when the size of the particles reaches the submicron or nanometer scale, the conductivity of a filled system is determined by the size of the space between conducting filler particles which electrons jump across according to a tunneling or emission mechanism of conductivity [26,27]. This tunneling effect can in fact be considered as a result of an equivalent contact resistor network. A strategy for appropriately modeling the tunneling effects will be to construct a number of “gap elements” around neighboring particles. Each gap will have a distance-dependent gap conductance to approximate the electronic tunneling effect. The gap conductance can be determined either from experiments or from fundamental quantum theories.

2. Methods

2.1. Contacting disk model

When materials are in contact, the temperature or voltage drop across the interface may be appreciable. This can be characterized by the thermal or electrical contact resistance, R , and

$$R = \frac{\Delta T}{q}, \quad (1)$$

where T represents the temperature or electrical potential and q is the heat flux or electrical current. Modeling the contact resistance requires the modeling of both transport phenomenon and contact mechanics. A direct simulation of the associated electromechanical or thermomechanical process is numerically difficult in the presence of interfacial contact. Therefore, instead of a coupled analysis, a simulation strategy employing the following three steps was used:

- (1) Dynamic deployment of randomly-arranged, impermeable circular disks.
- (2) Simulation of contact between deformable disks using an explicit finite element analysis.
- (3) Performing conduction analysis using an implicit finite element analysis.

In the first step, a system of impermeable, equisized circular disks was generated inside a unit cell. To avoid overlap between disks, a dynamic deployment algorithm was implemented in a standalone code. In the algorithm the initial velocities of overlapping disks allowed rigid body collisions when the disks met. The algorithm was run until no overlap was detected among the disks. The process typically required 10,000 numerical iterations, with a time step equivalent to the distance of 1/10th of the radius that a disk travels within each of the iterations. The particle size and number were predetermined in such a way that the initial volume fraction (the term “volume fraction” instead of “area fraction” is used throughout this paper to make it consistent with the three-dimensional case) was around 50%, well below the jamming fraction of rigid disks. Two different disk radii, 0.04 and 0.02, were investigated. Correspondingly, 100 and 400 disks were used in the study.

In the second step, the generated disks from the first step were discretized into a system of finite element elements using the commercial code COMSOL[®] [28]. The finite element mesh was first created on one disk and then replicated on the others. Each disk was divided into approximately 600 tetrahedron elements and 300 nodes, and therefore the overall size of the problem was between 30,000 and 120,000 nodes. To improve the computational accuracy during the contact analysis, a refined mesh was created at the outer layer of each disk. The thickness of the layer was set to 1/10th of the disk radius. The total number of

elements inside this layer was approximately 200, while a relatively coarse mesh was used for the rest of a disk. All the elements were assigned the same set of elastic material properties. The system was constrained inside a fixed, square domain of unit size. Each of the four sides of the square was compressed along either the x - or y -direction: the two vertical sides moved horizontally and the two horizontal sides moved vertically, whereas all the remaining degrees of freedom were fixed. The four sides were compressed at a constant speed so that the domain remained square during the procedure. Apparently, if the disks were initially at rest, the local density of disks would be higher near the boundary than in the interior, because the outside disks tended to gather together while the density of the inside disks remained unchanged. To minimize this possible inhomogeneity in the simulation, random initial velocities were assigned to the disks at the beginning to allow them to move around and adjust their locations throughout the simulation. ABAQUS EXPLICIT[®] [29] was used to model the contact interactions among disks, via an explicit direct integration. Because displacements and velocities in an explicit dynamic analysis are computed in terms of quantities that are known at the beginning of an increment, the global mass and stiffness matrices do not need to be formed and inverted, which means that each increment is computationally inexpensive compared to the increments in the implicit integration scheme. Pairwise contact interactions were assigned between the surface elements of the disks. Contact pairs were also defined between each individual disk and each side of the square domain. The collisions were considered to be fully elastic and no energy dissipations were assumed. To reduce the number of variables and the numerical complexity in the model, frictionless contact condition was assumed among all the contact surfaces. Poisson's ratio of the disk material was set to 0.5 (0.499 in reality) to avoid a change in area during the compression. Finally, when the disk system was loaded under a sufficiently small velocity, the result approached the quasi-static solution and the dynamic oscillations were negligible.

In the third step, the simulation results were immediately exported at the requested time intervals from step 2, each of which corresponded to a specific position of the domain walls during the compression, or specific volume fraction of the disks. The deformed finite element mesh along with the updated nodal positions at each time interval was then used to construct the conduction model in the subsequent analysis. In particular, a steady-state conduction model was developed based on the updated disk configurations obtained from step 2. The same contact definitions were retained, whereas all the kinetic degrees of freedom were removed and the temperature was the only remaining degree of freedom in the new analysis. A unit temperature was chosen on the top surface of the model while the temperature on the bottom was set to zero. Thermal conduction took place under the temperature gradient and the steady-state solution was sought by solving

Laplace's equation. The thermal expansion coefficient was chosen as zero to avoid material expansion in the presence of temperature gradient. It can be proved that the reactive heat flux is equivalent to the effective conductivity of such a system. The contact resistance was included in the simulation in the form of contact conductance, or "gap conductance", which could be dependent on either the contact pressure or the gap distance (i.e. the normal distance between two close surfaces). To minimize the computational effort in the analysis, a constant gap conductance was assumed once the contact surfaces became close enough. This was realized by checking if the gap distance was below a certain threshold, which was chosen as 0.1% of the disk radius. The implicit finite element scheme has been used in the conduction analysis because a direct, transient analysis using the explicit scheme in the current problem would otherwise require an extremely small time step due to the involvement of the contact resistance, and would therefore finding the solution would be much more costly. It should be pointed out that the equivalent conductivity obtained in this method can be used for both electrical and thermal analyses as long as the results are normalized against the material properties of the disks.

The above simulation procedure is shown schematically in Fig. 1A–C.

2.2. Overlapping disk model

Although the contact interaction is the main concern in the current study, a model constructed from overlapping disks was also used here for the purpose of comparison. The disks were modeled as randomly distributed overlapping circles, meaning that the centers of the disks were distributed randomly following a uniform probability density function, and no dynamic collision algorithms were implemented. A Boolean operation was then applied to the disks to obtain a union geometry. A finite element mesh was created on the resulting geometry as shown in Fig. 2. The internal lines in the geometry had been removed to avoid unnecessary mesh refinement near the locations of these lines. The local mesh density was curvature-dependent so that the numerical inaccuracy induced by the local singularities of the solution has been minimized. However, a curvature cutoff threshold was applied during the mesh generation

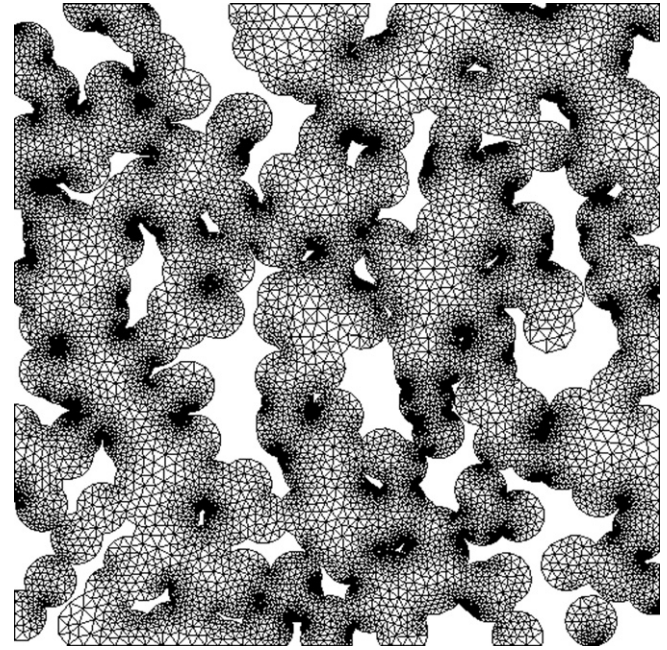


Fig. 2. Finite element mesh generated from the overlapping disk model; 100 disks are modeled.

to avoid excessive local elements. Boundary conditions similar to the contact model in step 3 were applied to compute the effective conductivity. The disk size was fixed throughout and the changing of volume fraction was made by varying the disk number. The simulation was run for 50 times at each volume fraction (or equivalently, each corresponding number of disks). The results were averaged at the end, and the means and the standard deviations were computed.

3. Results

3.1. Conduction in the contact model

The effective conductivity was studied as a function of volume fraction of disks in the contact model. Infinite gap conductance was assumed in the simulation. Fig. 3A shows the temperature field when the volume fraction of disks is 71%. Clearly, there is no conductive path across the system vertically at that volume fraction and the corresponding effective conductivity is zero. The temperature is strictly uniform for those disks connected to the top boundary constrained at a unit temperature. Meanwhile the temperature is zero for those disks not connected to the top boundary: either they form isolated clusters whose initial temperature is set to zero or they are connected to the bottom boundary constrained at a zero temperature. In addition, most disks remain circular as the contact interaction is rare. When the volume fraction increases to a certain level that is above the percolation threshold, at least one conductive path can be seen from the temperature distribution, as shown in Fig. 3B. Although some disks still form isolated clusters whose temperature is uniform inside, there clearly exist some locations where the

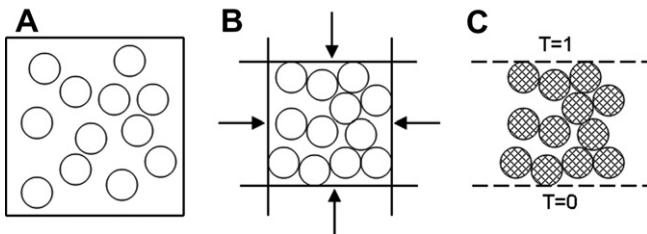


Fig. 1. Schematic of the simulation procedure: (A) step 1: dynamic collision simulation for generating impermeable, random disks; (B) step 2: compression of the disk system; and (C) step 3: conduction analysis.

color variations inside the disks reflect the vertical temperature gradients across the system. It can also be seen that some disks have been elastically deformed due to the mechanical contact between them. Fig. 4 shows the deformed disk shapes along with the finite element mesh during the compression; the contact regions can be clearly seen. When the volume fraction further increases to 83% as shown in Fig. 3C, the disks are interconnected everywhere and the temperature gradients are nearly the same. When the volume fraction further increases to 97% as shown in Fig. 3D, the elastic deformation becomes so significant that the disks have been compressed into hexagons. The increased contact areas and reduced void spaces make the system behave like a homogeneous material. The temperature gradient and hence heat flux is almost uniformly distributed from top to bottom.

The relationship between the conductivity and the volume fraction was obtained for two different sizes of disks: (1) 100 disks of radius 0.04 and (2) 400 disks of radius

0.02. The results are shown in Fig. 5, in which the effective conductivity is normalized by the conductivity of the material used for the disks. It is seen that the disks start to form conductive paths when the volume fraction is above a certain threshold located between 70% and 75%. This threshold is below the close packing limit for random disks in an infinite system, which is between 82% and 89% [30]. This is because a relatively small number of disks was used in this study and the scaling effect played a significant role. Above the threshold, the conductivity is almost a linear function of volume fraction. It seems that the simulation results do not display much difference for different sizes of disks, especially when the volume fraction is well above the packing limit. This is because the disks were constrained against each other through contact interfaces and the variations in their spatial locations were limited. By comparison, the disks in the overlapping scenarios were allowed to move freely. Therefore we conclude that 400 disks is a reasonable

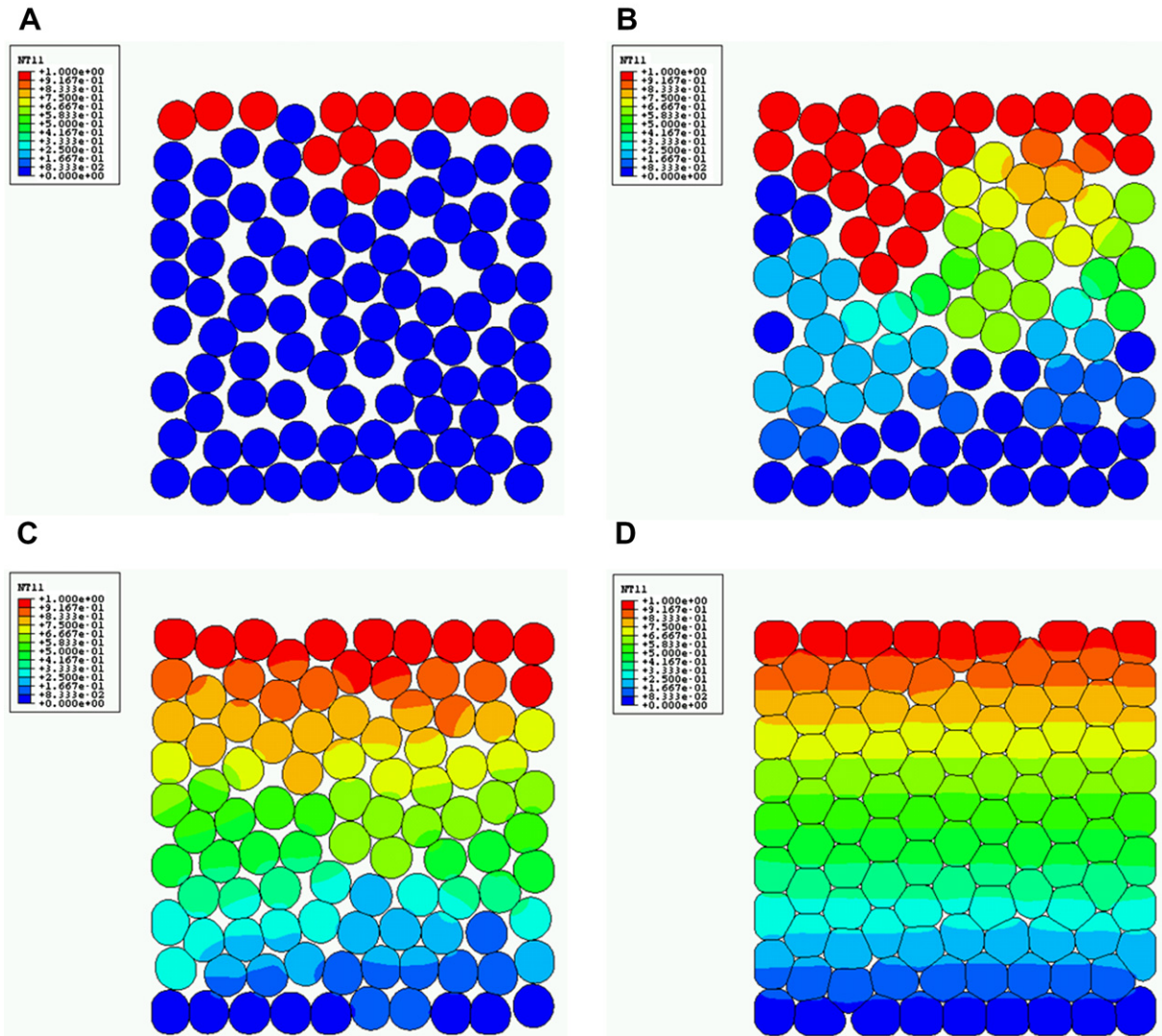


Fig. 3. Temperature gradient in the contact model under various volume fractions: (A) 71%; (B) 77%; (C) 83%; and (D) 97%. The domain sizes are enlarged to make them look the same.

number for use in the simulation, and the results should reflect the fundamental features of the problem of interest.

3.2. Conduction in the overlap model

The relationship between the effective conductivity and the volume fraction has also been investigated for overlapping disks. In the simulation, 400 disks of radius 0.02 were used to make the parameters consistent with those used in the contact model. In Fig. 6, it is clear that the conductivity increases with the volume fraction, following an approximately power-law curve. The predicted percolation threshold is located in the vicinity of the 60% volume fraction, which is much lower than the theoretical prediction of 68% in an infinite system [31]. This is because of the scaling effect induced by the small number of disks (400) in this study. It can be expected that as the disk number increases to infinity, this threshold should approach the theoretical

prediction. The standard deviations of the results are also presented here, which are seemingly not very significant, but in fact much greater than those in the contact model, for the reason stated above.

3.3. Comparisons between the contact model and the overlap model

The simulation results for the contact model and the overlap model are combined in Fig. 7. Clearly the overlapping model predicts a much lower percolation threshold. However, the thresholds converge to common values when the volume fraction approaches to 100%. This can be explained as follows: in the vicinity of the percolation threshold, the contact areas are much smaller than the disk diameter and hence the effect of the contact area on the overall conductivity is predominant. In the contact model, we can estimate the contact length as a function of volume fraction, assuming an idealized contact situation shown in Fig. 8. From elementary trigonometry and algebra, it can be proved that

$$\varepsilon = \frac{a}{b} = 1 - \sqrt{\frac{1-f}{1-\frac{\sqrt{3}\pi}{6}}}, \quad \frac{\sqrt{3}\pi}{6} \leq f \leq 1, \quad (2)$$

where a is the contact length, b is the side length of the hexagon shown in Fig. 8 and f is the volume fraction of disks. The constant $\sqrt{3}\pi/6$ ($\approx 90.7\%$) is the packing limit for the crystal packing of disks. On the other hand, we can also estimate the mean “overlap length” (here defined as the length connecting the two intersection points of the overlapping circles) to be a function of volume fraction as shown in Fig. 9. The disks were assumed to be in a honeycomb lattice structure so that the overlap length was the same everywhere. The analytical result is presented below:

$$f = \varepsilon + \frac{1}{\sqrt{3}} [\varepsilon^2 + 3] \left[\frac{\pi}{6} - \tan^{-1} \left(\frac{1}{\sqrt{3}} \varepsilon \right) \right], \quad 0 \leq \varepsilon \leq 1. \quad (3)$$

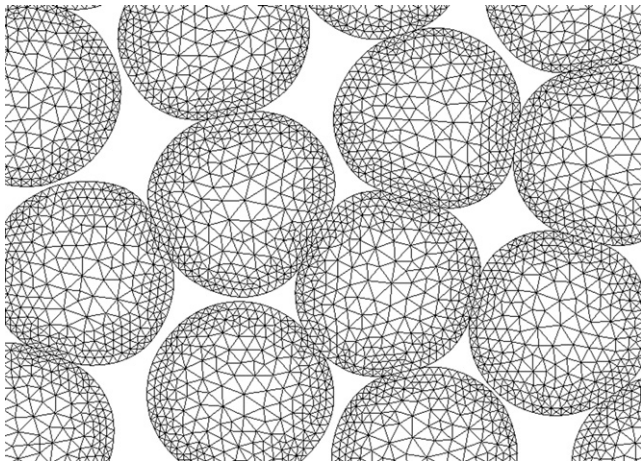


Fig. 4. Deformed mesh of the contact model under a volume fraction of $\sim 80\%$.

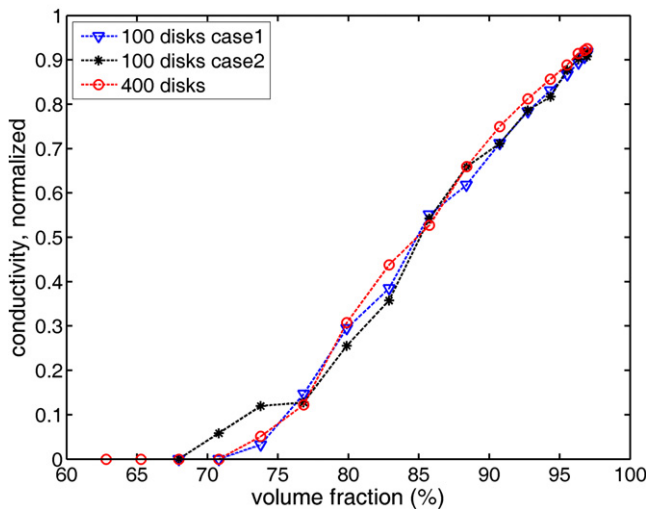


Fig. 5. Effective conductivity as a function of volume fraction in the contact model.

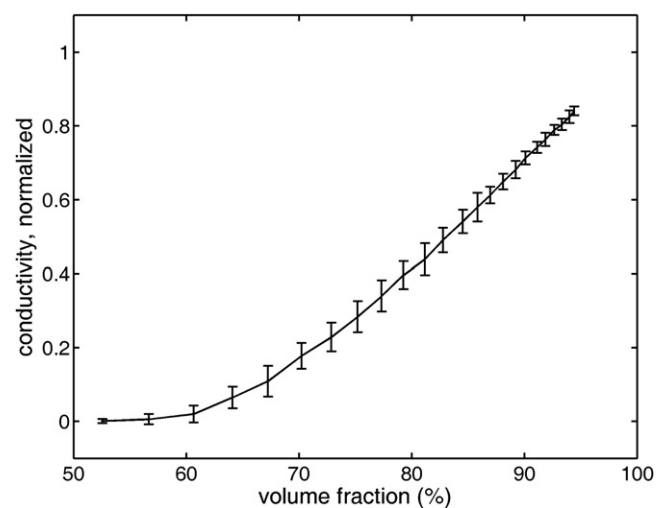


Fig. 6. Effective conductivity as a function of volume fraction in the overlap model.

The functions in Eqs. (1) and (2) are plotted in Fig. 10. It can be seen that both the normalized contact length and overlap length start from 0 at the crystal packing limit, monotonically increase with the volume fraction, and end at 1 for 100% volume fraction. Apparently, the contact length in the contact model is consistently shorter than the length in the overlap model. This is because the deformed boundaries of two contacting disks must be tangential to each other, whereas there is no such restriction for overlapping disks. Consequently, the reduced contact area leads to a reduced conductivity in the contact model. However, when the volume fraction approaches 100%, the two lengths in Fig. 10 come close to each other and the corresponding effective conductivities also converge.

Fig. 7 also shows for comparison two additional curves obtained from the effective medium theories. One curve is obtained from Maxwell's approximation [32]

$$K = \frac{f}{2 - f}, \tag{4}$$

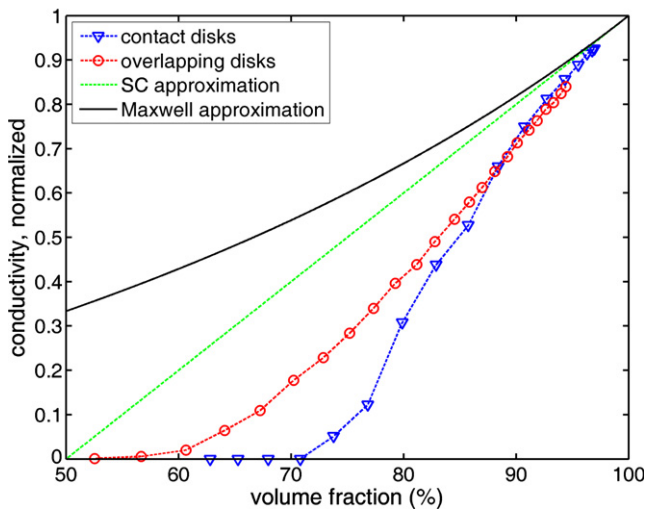


Fig. 7. Comparison of the simulation results between the contact model and the overlap model.

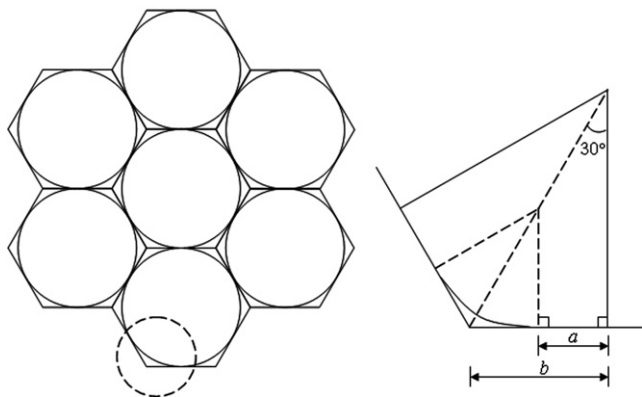


Fig. 8. Schematic of the contact length in an idealized contact situation.

and the other is obtained from the self-consistent (SC) approximation [33], i.e.

$$K = 2f - 1, \tag{5}$$

where K is the effective conductivity normalized by the conductivity of disks and f is the volume fraction. Clearly, both approximations overestimate the conductivity compared to the simulation results. In addition, The SC approximation predicts a percolation threshold of 50%, which is much lower than the actual value. Meanwhile Maxwell's approximation is unable to provide any reasonable estimate for the percolation threshold.

Therefore, using the overlap model or the effective medium theories to model contacting particles typically overestimates the effective conductivity. This has been confirmed by the experimental results reported in Wang et al.'s work [14], in which the predicted conductivities using permeable particle models were generally much higher than the experimental measurements for graphite particles in Li-ion electrodes.

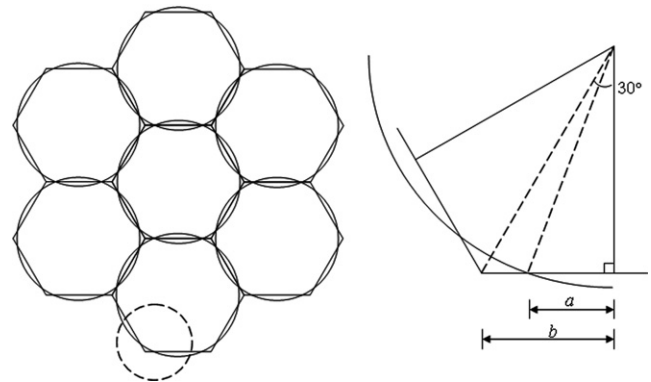


Fig. 9. Schematic of the overlap length in an idealized overlap situation.

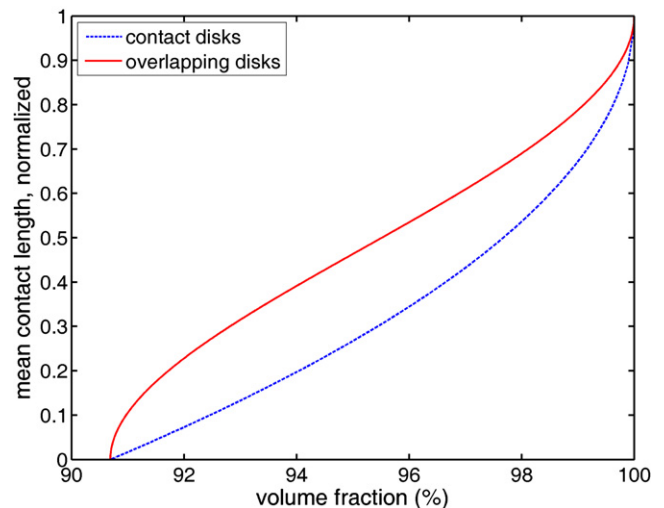


Fig. 10. Contact and overlap lengths as functions of volume fraction.

3.4. Effect of gap conductance

All the above results and discussions were based on the assumption of infinite gap conductance, or zero contact resistance, in which the contact between the deformable bodies alters the conductivity through the change in the contact area alone. Incorporation of a realistic, finite gap conductance and hence a nonzero contact resistance will certainly reduce the effective conductivity. A quantitative relationship has been obtained for a special case of 100 disks and 90% volume fraction, as shown in Fig. 11. The disk configurations were maintained the same and the gap conductance was the only variable. As expected, the results reach a plateau of 0.61 when the gap conductance exceeds a value close to 1.0×10^3 . If the gap conductance is relatively small, the conductivity of the entire system is dominated by the conduction across the contact interface and should also be small. For example, for unit gap conductance, the effective conductivity of the system is only 0.03, a reduction of 20 times in comparison with the result assuming zero contact resistance. The overall shape of the curve is inherently nonlinear, because two different parameters – the conductivity of the disk material and the gap conductance – both play important roles in the overall conductivity. Although the result in Fig. 11 was obtained from a special case with 90% volume fraction, similar results were observed in other situations with different volume fractions and configurations.

4. Conclusions

A general simulation technique has been proposed to compute the effective conductivity of contacting particles as opposed to overlapping ones. A contact model is introduced to include not only the contact mechanics but also the gap conductance across the particle–particle interface. The analysis is performed through several subsequent steps using a finite element approach. It is shown that both the

contact area and the contact resistance have significant effects on the conductive properties when the volume fraction is near the packing limit of rigid disks. The simplification of the contacting particles using the overlap assumption or the effective medium theories generally overestimates the effective conductivity. This has been confirmed by the experimental results found in the literature. When the volume fraction is sufficiently high, however, all the results agree well. Although the simulations are performed based on idealized, equisized circular disks, the same technique can be extended to other problems involving noncircular, polydisperse particles in either two- or three-dimensions. Future work will also include modeling the frictional contact and possibly the pressure-dependent contact resistance.

It should be pointed out that, to the author's knowledge, the overlapping disk model is probably the best of the existing theoretical models for comparing the results with the contact model developed here (in the limiting case of superconducting interface). Because the mechanism of the interfacial resistance involved in the current research and those discussed in the literature are physically different, as mentioned in Section 1, a direct comparison of the computational results with the theoretical predictions made by other researchers working on the inclusion–matrix interfacial effects will be difficult and possibly misleading. Nevertheless a qualitative comparison should be very important in the future work, especially for the development of a more advanced model to incorporate both the inclusion–matrix and inclusion–inclusion interfacial contact situations.

References

- [1] Cheng X, Sastry AM. *Mech Mater* 1999;31:765–86.
- [2] Mohanty S, Sharma MM. *Phys Lett A* 1991;154:475–81.
- [3] Torquato S. *Random heterogeneous materials*. New York: Springer Verlag; 2002.
- [4] Cheng X, Sastry AM, Layton BE. *ASME J Eng Mater Technol* 2001;123:12–9.
- [5] Wang HY, Yoshio M, Abe T, Ogumi Z. *J Electrochem Soc* 2002;149:A499–503.
- [6] Okada H, Fukui Y, Kumazawa N. *Comput Struct* 2001;79:1987–2007.
- [7] Sigmund O. *J Mech Phys Solids* 2000;48:397–428.
- [8] Yi YB, Sastry AM. *Proc Royal Soc Lond A: Math Phys Sci* 2004;460:2353–80.
- [9] Kirkpatrick S. *Rev Mod Phys* 1973;45:574–88.
- [10] Yi YB. *Phys Rev E* 2006;74 [Art. No. 031112].
- [11] Wang XF, Wang YL, Jin ZH. *J Mater Sci* 2002;37:223–7.
- [12] Pike GE, Seager CH. *Phys Rev B* 1974;10:1421–34.
- [13] Kepler KD, Vaughney JT, Thackeray MM. *Electrochem Solid State Lett* 1999;2:307–9.
- [14] Wang CW, Yi YB, Sastry AM, Shim J, Striebel KAJ. *Electrochem Soc* 2004;151:1489–98.
- [15] Maleki H, Selman JR, Dinwiddie RB, Wang H. *J Power Sources* 2001;94:26–35.
- [16] Striebel KA, Sierra A, Shim J, Wang CW, Sastry AM. *J Power Sources* 2004;134:241–51.
- [17] Yi YB, Berhan L, Sastry AM. *J Appl Phys* 2004;96:1318–27.
- [18] Berhan L, Yi YB, Sastry AM, Munoz E, Selvidge M, Baughman R. *J Appl Phys* 2004;95:4335–45.

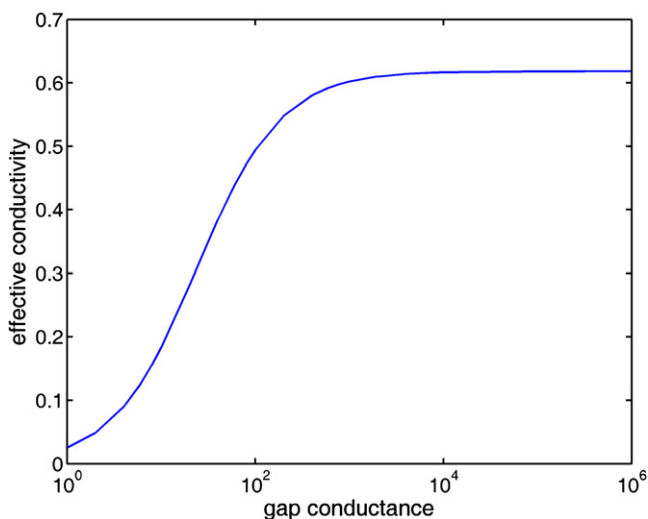


Fig. 11. Effective conductivity as a function of gap (contact) conductance.

- [19] Berhan L, Sastry AM. *Phys Rev E* 2007;75 [Art. No. 041120].
- [20] Berhan L, Yi YB, Sastry AM. *J Appl Phys* 2004;95:5027–34.
- [21] Torquato S, Rintoul MD. *Phys Rev Lett* 1995;75:4067–70.
- [22] Miloh T, Benveniste Y. *Proc Roy Soc Lond A* 1999;455:2687–706.
- [23] Wei EB, Poon YM. *Phys Lett A* 2006;359:685–92.
- [24] Benveniste Y. *J Mech Phys Solids* 2006;54:708–34.
- [25] Yi YB, Wang CW, Sastry AM. *ASME J Eng Mater Technol* 2006;128:73–80.
- [26] Dawson JC, Adkins CJ. *J Phys-Condens Mat* 1996;8:8321–38.
- [27] Li L, Morris JE. *IEEE Trans Compon Packaging Manuf Technol Part A* 1997;20:3–8.
- [28] COMSOL Multiphysics® 3.3 User's Manual. COMSOL Inc.; 2006.
- [29] Abaqus/Standard/Explicit® version 6.0 User's Manual. ABAQUS Inc.; 2005.
- [30] Berryman JG. *Phys Rev A* 1983;27:1053–61.
- [31] Quintanilla J, Torquato S. *Phys Rev E* 1996;54:5331–9.
- [32] Maxwell JC. *Treatise on electricity and magnetism*. Oxford: Clarendon Press; 1873.
- [33] Landauer R. *J Appl Phys* 1952;23:779–84.